A NOVEL APPROACH FOR TURBULENCE MODELING OF WAVY STRATIFIED TWO-PHASE FLOW

M. Benz, T. Schulenberg
Institute for Nuclear and Energy Technologies
Karlsruhe Institute of Technology
Hermann-von-Helmholtz-Platz 1, 76344 Eggenstein-Leopoldshafen, Germany
matthias.benz@kit.edu; thomas.schulenberg@kit.edu

ABSTRACT

A new numerical model for stratified two-phase flows with wavy interface is derived in this study. Assuming an equilibrium condition between turbulent kinetic energy, potential energy and surface energy, the turbulent length scale in the inner region of a two-layer turbulence approach can be described by a statistical model to account for the influence of the waves. The average wave number, which is an input parameter to this model, is taken from wave spectra. They can be predicted from a Boltzmann statistic of turbulent kinetic energy. The new turbulence model is compared with the two-phase k-ϵ-turbulence model. Time averaged flow properties calculated by the new approach, such as velocity, turbulence and void profiles, are shown to be in good agreement with experimental data.

KEYWORDS
Stratified two-phase flow, turbulence, waves, wave spectra, CFD

1. INTRODUCTION

Stratified wavy gas/liquid-two-phase-flow can be found in many engineering applications such as pipe or channel flows in a steam cycle. In pressurized water reactors, the prediction of horizontal stratified flows became important in case of Loss-of-Coolant-Accidents when coolant has to be injected into the reactor pressure vessel through the hot leg by the Emergency Core Cooling System (ECCS) to flood the reactor core from top. Liquid coolant meets then with vapor coming from the reactor core, forming a countercurrent, stratified two-phase flow. The description of those flows is much more difficult compared with single-phase flows because interfacial transfer processes of mass, momentum and heat have to be considered additionally. Furthermore, shear stresses at the interface lead to flow instabilities in the form of surface waves.

Depending on the flow velocity, we distinguish between subcritical and supercritical flow, which are determined by the Froude number. It describes the ratio of inertia to gravity forces or, in other words, the ratio of flow velocity to the phase velocity of surface waves. For Froude numbers larger than unity, inertia dominates and the flow is supercritical. In this regime, waves with small amplitude only can be observed. If the flow is subcritical ($Fr < 1$), gravity forces dominate and waves with much larger amplitude occur. During the transition from super- to subcritical flow, the water depth rises abruptly. This phenomenon is called a hydraulic jump. Another phenomenon, which occurs in countercurrent stratified two-phase flow, is the so-called countercurrent flow limitation (CCFL). At sufficient gas velocities, shear stresses at the interface are causing parts of the liquid flow to be reversed near the interface and to flow backwards in the direction of the gas flow. Further increase of the gas velocity, finally leads to total flow reversal and liquid does not reach the end of the pipe anymore. In case of the ECCS in a nuclear power plant, top flooding of the reactor core would be inhibited.

According to Rashidi et al. [1], turbulence in the liquid phase is of significant importance for interfacial transport in stratified flows. This was the reason for many investigations on turbulent structures near the interface. However, turbulence of waves is still not fully understood mainly because of experimental constraints near the wavy interface.

Nevertheless, Komori et al. [2] found from their experimental results in open channel flows that large eddies, generated at the wall, renew the free surface and are then reflected back into the bulk flow. Same results were also reported by Rashidi and Banerjee [3].

Rashidi et al. [1] showed that, eddies are also generated at interfaces on which shear was imposed and that their main characteristics are similar to those generated at the wall. Later, Rashidi et al. [4] investigated the influence of surface waves, generated by a mechanical wavemaker, on turbulence of the liquid phase. They reported that the turbulence mechanisms in presence of surface waves are comparable to that in the case of non-wavy interfaces. However, they found a direct impact of the wave amplitude on the eddy ejection frequency. Increasing the wave height also increases the ejection of eddies. On the other hand, there is no direct dependency of the ejection frequency on the wave frequency and therefore on the wavelength. Furthermore, an acceleration of the fluid from the wave trough to the wave crest has been observed with an increase of the fluid velocity and turbulence under the crest and a decrease under the trough.

Different from the study mentioned above, waves are generated by shear stresses at the interface of a gas-liquid flow in the work of Lorencez et al. [5]. Their data, however, showed similar effects with turbulent fluctuations also ejected from the liquid interface, which then travel into the bulk flow and increase the turbulent mixing effect. Therefore, they suggest that the generation of turbulent eddies at the interface is the main mechanism of interfacial momentum transfer.

Stäbler [6] used the test facility of Gargallo et al. [7] for his measurements to provide detailed local experimental data of countercurrent stratified air-water flow with wavy interface for the development of new modeling approaches. This data showed that the velocity in horizontal direction decreases near the interface due to high interfacial shear stresses imposed by the gas flow. The vertical component also gets damped at the interface, but at much smaller rates than horizontal one. On the other hand, turbulent fluctuations increase rapidly near the interface. According to Stäbler, this is because of the deceleration of the liquid flow in horizontal and the motion of the surface waves in vertical direction. Based on an equilibrium state between turbulent kinetic energy and potential energy of the fluid particles, he derived a statistical model for the description of the void profiles. This model shows very good agreement with deviations less then 5% for partly reversed flow and less than 9% for subcritical flow. Within the supercritical flow regime, agreement with experimental results was not as good, but still less than 17% deviation only.

Besides these experimental investigations, also some numerical studies on stratified two-phase flows can be found in literature. Among others (e.g. Daly and Harlow [8], Akai et al. [9], Lorencez et al. [5]), the work of Berthelsen and Ytrehus [10] is interesting to mention. Using the level set method, they simulated a stratified gas-liquid pipe flow. A modified two-layer-turbulence approach has been applied to include the effect of surface waves. Originally, Chen and Patel [11] developed the two-layer-turbulence model to overcome the shortcomings of the standard-k-ϵ-model near walls. Therefore they divided the flow into two regions. In the outer region further away from physical boundaries, such as walls or free surfaces, the standard-k-ϵ turbulence model was applied, while turbulence in the viscous-affected inner region was modeled by a simpler one-equation k-l-model. To account for the enhancement of turbulence at the interface due to waves, Berthelsen and Ytrehus introduced an additional displacement height in the turbulent length scale of the inner region, which is a function of an equivalent roughness parameter.

Höhne et al. [12] derived a CFD model for free surface flows using a two-fluid formulation. Defining an interfacial area density together with blending functions, they are able to account for different morphological forms (bubbles, droplets, continuous phase) for which different interfacial drag models are used. Furthermore, the influence of small waves, which are smaller than the grid size, is considered by an additional production term in the transport equation of the turbulent kinetic energy. First validation of the model against experimental data of Fabre et al. [13] and Vallée et al. [14] showed better results compared to three standard turbulence models. But there is still some deviation compared to experimental data.

Finally, Wintterle et al. [15] developed a phase exchange model based on the void model of Stäbler [6]. They introduced an additional dispersion force to their two-fluid model to model the smearing of the wavy interface due to a statistical time averaging of the surface waves. Furthermore, a production term was added to the dissipation equation of the k-ω-turbulence model to account for turbulence damping in the phase interaction zone.

In stratified flows, turbulence is not only controlled by shear stresses at the walls but also by the interaction between turbulence and interfacial waves. In principle, the wavy interface can be described with the volume-of-fluid method, resolving each wave in detail. Such methods, however, require long CPU times because of extremely small grid sizes, while the details of the waves are usually not of engineering interest. Instead, using RANS approaches on a coarser grid together with a statistical model describing these waves would be desirable. Such a model can be derived based on an equilibrium state between turbulent kinetic energy, potential energy and surface energy. The simple one-equation turbulence formulation in the inner wave region of the two-layer turbulence approach offers an easy way to include the effects of interfacial drag and waves on the turbulence in two-phase stratified flows without a need to model drag forces.

2. WAVE STATISTICS

Similar to Stäbler [6], a statistical model for the description of surface waves can be derived from the equilibrium between turbulent kinetic energy, potential energy and surface energy. Surface energy has been neglected by Stäbler [6], which we expect to be the reason for the deviation between the results of his void model and his experimental data in supercritical flows. In such a flow, waves with relative small amplitude occur and capillary forces become dominant. Therefore, surface energy has been included in this study.

2.1. Wave Spectra

As confirmed experimentally by Stäbler [6], the local velocity u follows a Gaussian distribution with the variance $\overline{u'^2}$ and the mean velocity $\bar{u}$:

$$P(u) = \frac{1}{\sqrt{2\pi\overline{u'^2}}} \exp\left(-\frac{(u-\bar{u})^2}{2\overline{u'^2}}\right) \tag{1}$$

Extension by the density $\rho/2$ and generalization to three dimensions yields a Boltzmann distribution for the turbulent kinetic energy density E_{kin}:

$$P(E_{kin}) = \frac{1}{2\rho k} \exp\left(-\frac{E_{kin}}{2\rho k}\right) \tag{2}$$

where $\rho k = \alpha\rho_G k_G + (1-\alpha)\rho_L k_L$and α denotes the void fraction.

The fluid can use turbulent kinetic energy to increase the potential energy density ΔE_{pot} by lifting up fluid from position y to $y + dy$, and to increase surface energy density ΔE_{surf}. The probabilities that the kinetic energy is sufficient for each of the two mechanisms are:

$$P(\Delta E_{pot}) = \frac{1}{2\rho k} \exp\left(-\frac{\Delta E_{pot}}{2\rho k}\right) \tag{3}$$

$$P(\Delta E_{surf}) = \frac{1}{2\rho k} \exp\left(-\frac{\Delta E_{surf}}{2\rho k}\right) \tag{4}$$

where $\Delta E_{pot} = (\rho_L - \rho_G) g dy$ and $\Delta E_{surf} = \sigma q^2 dy$ (Benz et al. [16]). We denote g as the acceleration of gravity, ρ_G as the gas density and σ as the surface tension.

Both transfer mechanisms are always acting simultaneously, which leads to the probability function of the total wave energy ΔE:

$$P(\Delta E) = P(\Delta E_{pot}) * P(\Delta E_{surf}) = \frac{1}{2\rho k} \exp\left(-\frac{\Delta E_{pot} + \Delta E_{surf}}{2\rho k}\right) \tag{5}$$

The integral over the total energy spectrum has been normalized to one.

Eqn. (5) describes the interaction between turbulence and the wave. The wave gets its energy from a kind of energy reservoir ρk, which is fed from both phases. Unlike Stäbler [6], who only used the density and the turbulent kinetic energy of the liquid phase in eqn. (2) because of difficulties in measuring gas phase velocities near the interface, we are using the total kinetic energy with this formulation. Thus, we are including also the turbulent kinetic energy of the gas phase.

Integrating the energy densities over the wavy interface, we can derive a similar probability for energies per unit (undisturbed) surface area, which shall enable us to predict wave spectra. We denote these integrals of the kinetic, the potential and the surface energy densities as E_t, E_{pot} and E_{surf}, respectively. Similar to eqn. (5), the probability function of the total wave energy $E=E_{pot}+E_{surf}$ per unit surface area can be written as:

$$P(E)dE = \left(P(E_{pot}) * P(E_{surf})\right) dE = \frac{1}{E_t} \exp\left(-\frac{E_{pot} + E_{surf}}{E_t}\right) dE \tag{6}$$

where $E_{pot} = \frac{1}{4}\Delta\rho g h^2$ and $E_{surf} = \frac{1}{4}\sigma q^2 \bar{h} h$, with the wave amplitude h and the spectrum averaged wave amplitude $\bar{h} = H/2$. E_t is the mean turbulent kinetic energy of the wavy layer of the thickness H. In case of constant turbulent kinetic energy, it can be approximated as:

$$E_t = \int_{-h}^{h} \rho k(y) dy \approx 2\rho k \bar{h} \tag{7}$$

Like eqn. (5), eqn. (6) is normalized to one ($\int_0^\infty P(E)dE = 1$).

The wave amplitude h is a function of wave number q. The product of h and q, which we denote here as the wave aspect ratio A ($A = hq$), has an upper limit of 0.5 according to the second order wave theory of Stokes. Multiplying eqn. (12) by the derivative of the wave energy dE/dq and using the assumption that A is constant, yields to the wave number spectrum:

$$P(q)dq = P(E)\frac{dE}{dq}dq = \frac{1}{E_t}\left[\frac{\Delta\rho g A^2}{2q^3} + \frac{\sigma A\bar{h}}{4}\right]\exp\left(-\frac{\Delta\rho g\frac{A^2}{q^2} + \sigma q A\bar{h}}{4E_t}\right)dq \quad (8)$$

Note that the first term in the square brackets in eqn. (8), which is the derivative of the potential energy, is positive due to normalization of the gravity wave spectrum.

Unfortunately, such spectra of wave numbers have hardly been measured. Instead, wave frequency spectra have been measured, which are technically much easier to obtain. Generally, the spectrum of the wave frequency f can be derived from the wave number spectrum as:

$$P(f)df = P(q)\frac{dq}{df}df \quad (9)$$

The derivative dq/df in eqn. (9) depends on the wave dispersion relation, on the Doppler effect, and thus also on wave reflections at sidewalls, which differ for individual flow regimes. As mentioned above, we need to distinguish between subcritical and supercritical flows depending on the Froude number. Neglecting capillary forces, it is defined as the ratio between inertia and gravity forces:

$$Fr = \frac{u}{\sqrt{g\delta}} \quad (10)$$

with the flow velocity u and the mean water depth δ.

In subcritical flow, where $Fr < 1$, waves are travelling in the direction of the driving force (e.g. wind) with the wave phase velocity c and in other directions depending on reflections. We call them running waves. In such flows, the observed wave frequency f is different from the intrinsic wave frequency because of the Doppler effect. The observed frequency can be determined as:

$$f = \frac{q}{2\pi}(c - u) \quad (11)$$

Then, the derivative dq/df in eqn. (9) can be determined from eqn. (11) for subcritical flows as:

$$\frac{dq}{df} = \frac{2\pi}{(c - u) + q\frac{dc}{dq}} \quad (12)$$

The wave phase velocity c can be calculated in good approximation from linear wave theory. Assuming deep water, we get for gravity-capillary waves:

$$c_{deep} = \sqrt{\frac{g}{q} + \frac{\sigma q}{\rho_L}} \quad (13)$$

In supercritical flow ($Fr > 1$), waves are travelling downstream with the velocity u of the flow. They are not running in a coordinate system moving with the flow velocity, but just decay exponentially. We call them frozen waves. For such waves, $c = 0$ and the observed frequency and the derivative dq/df are determined as:

$$f = \frac{qu}{2\pi} \tag{14}$$

$$\frac{dq}{df} = \frac{2\pi}{u} \tag{15}$$

In a supercritical flow close to $Fr = 1$, however, we observe also running waves. We can explain this phenomenon by including the capillary term in the denominator in eqn. (10). In the case of shallow water, we can write the phase velocity $c_{shallow}$ including capillary forces as:

$$c_{shallow} = \sqrt{g\delta + \frac{\sigma q^2 \delta}{\rho_L}} \tag{16}$$

The ratio of the flow velocity u to the phase velocity yields then the extended Froude number Fr^*:

$$Fr^* = \frac{u}{c_{shallow}} = \frac{u}{\sqrt{g\delta + \frac{\sigma q^2 \delta}{\rho_L}}} \tag{17}$$

Using eqn. (17), we find that the flow is supercritical for $q < \sqrt{\rho_L(u^2 - g\delta)/\sigma\delta}$, i.e. in the lower spectrum of wave numbers, while for the flow is subcritical if $q > \sqrt{\rho_L(u^2 - g\delta)/\sigma\delta}$, i.e. in the upper spectrum of wave numbers. For the prediction of the frequency spectrum, frozen waves and running waves must be superimposed. It must be noted that the shallow water phase velocity $c_{shallow}$ must be used in eqn. (12) to predict the spectrum of the running waves in this case.

2.2. Void Distribution

Deriving the void profile from eqn. (5), we need to consider that liquid displaces other liquid, like the Pauli exclusion principle in particle physics. The probability P_1 that fluid transfers its kinetic energy to potential energy and to surface energy, can be written as the product of the probability that liquid exists at a vertical position y (which is identical to the liquid volume fraction 1-α), the probability of the existence of an empty space (or void α) at $y + dy$, and the probability that the required energy can be provided by the turbulent kinetic energy of the liquid:

$$P_1 = [1 - \alpha(\mathrm{y})]\alpha(\mathrm{y} + \mathrm{dy})P(\Delta E) \tag{18}$$

After linearization for small dy, eqn. (18) yields to:

$$P_1 = [1 - \alpha(\mathrm{y})]\alpha(\mathrm{y} + \mathrm{dy})\frac{1}{2\rho k(y)}\left[1 - \frac{\Delta\rho g dy}{2\rho k(y)} - \frac{\sigma q^2 dy}{2\rho k(y)}\right] \tag{19}$$

Similarly, the probability P_2 that potential and surface energies are transferred back to kinetic energy is:

$$P_2 = \alpha(y)[1 - \alpha(y + dy)]\frac{1}{2\rho k(y)} \tag{20}$$

Assuming that both probabilities must be the same in a mechanical equilibrium and by neglecting higher order terms, an expression for the gradient of the void fraction distribution can be derived as:

$$\frac{d\alpha}{dy} = \alpha(y)[1 - \alpha(y)]\frac{\Delta\rho g + \sigma q^2}{2\rho k(y)} \tag{21}$$

An average height H of the wavy interface can be estimated by linear extrapolation of eqn. (21) at $\alpha = 0.5$:

$$H = \frac{1}{\left.\frac{d\alpha}{dy}\right|_{\alpha=0.5}} \tag{22}$$

Integration of eqn. (21) yields to the void fraction distribution over the channel height:

$$\alpha(y) = \frac{1}{1 + \exp\left(-\int_{y_M}^{y} \frac{\Delta\rho g + \sigma q^2}{2\rho k(y)} dy\right)} \tag{23}$$

with the time-averaged position of the interface y_M. This type of probability function is a Fermi-Dirac distribution.

In eqns. (21) and (23), the wave number q is an input parameter. Assuming that gravity waves contribute mostly to the vertical void profile while the smaller capillary waves are just riding on the gravity waves, contributing only little to the void distribution, it can be calculated from eqn. (8), averaged over the spectrum of gravity waves ($\sigma = 0$) as:

$$\bar{q}_{grav} = \int_0^\infty q P_{grav}(q) dq = \sqrt{\frac{\pi}{4}\frac{\Delta\rho g A^2}{E_t}} \tag{24}$$

where $P_{grav}(q) = \frac{1}{E_t}\frac{\Delta\rho g A^2}{2q^3}\exp\left(-\frac{\Delta\rho g A^2}{4E_t q^2}\right)$.

2.3. Validation of Wave Statistics

2.3.1. Validation of wave spectra

The predicted wave spectra are validated against the experimental results of Stäbler [6]. Fig. 2 shows the measured frequency spectrum of a subcritical, partly reversed flow (data point 5 in [6]). The frequency spectrum shown here has been predicted using the deep water approach. Both spectra are in very good agreement if f > 1.6 Hz. The calculated spectrum is not shown for frequencies lower than 1.6 Hz, because these waves are more and more influenced by the channel ground and, therefore, the used deep water assumption is not valid anymore.

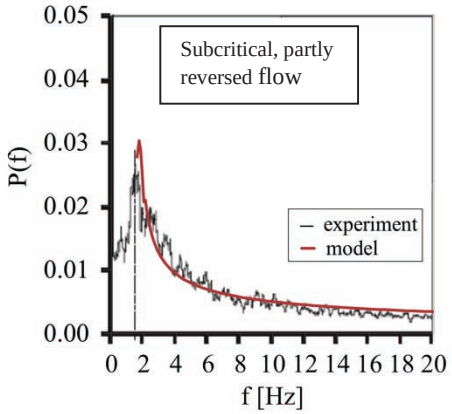

Figure 2. Predicted and measured frequency spectrum of a subcritical, partly reversed flow.

In supercritical flow, the spectrum predicted by the statistical model agrees also well with the experimental results of Stäbler [6] as shown for data point 74 with Fr = 1.36 in Fig. 3a). Frozen and running waves can clearly be distinguished in the wave number spectrum, Fig. 3b). The limit between both regions equals $\sqrt{\rho_L(u^2 - g\delta)/\sigma\delta}$. In the frequency spectrum, however, frozen and running waves are superimposed up to a frequency of 31 Hz. Which corresponds with the limit wave number according to eqn. (20), and pure running waves can be measured only beyond 31 Hz.

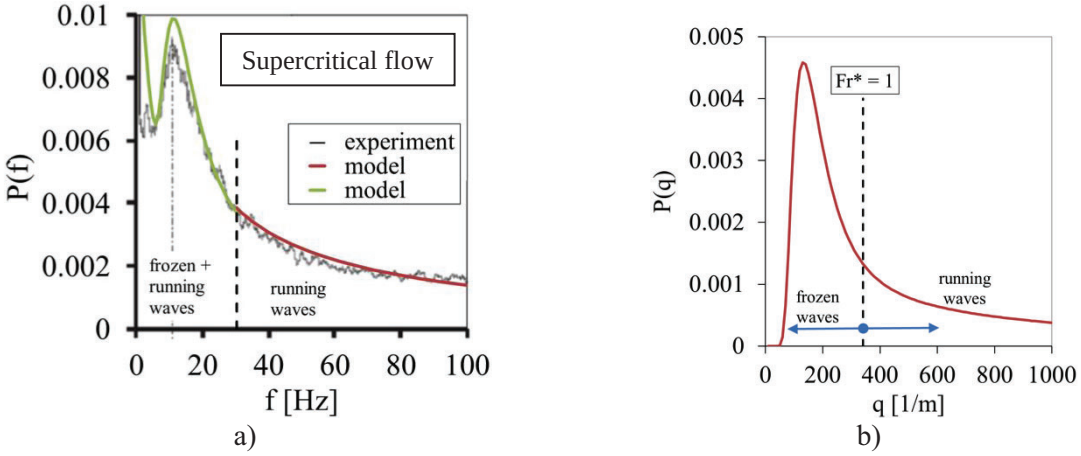

Figure 3. Frequency spectrum (a) and wave number spectrum (b) of a supercritical flow.

2.3.2. Validation of the void distribution model

For validation of the void distribution model, the void distribution is calculated from eqn. (23) and is compared with the measured void profiles from the experiments of Stäbler [6]. The turbulent kinetic energy and the wave aspect ratio are taken from the measurements. The wave number q is calculated from eqn. (24). Both the results of the newly developed void model and those of the model of Stäbler [6] are shown in Fig. 1a) for a subcritical, partly reversed flow (data point 10 in [6]) and in Fig. 1b) for a supercritical flow (data point 54). In subcritical flow, the calculated void profiles of both models are nearly identical, because waves are relatively high and therefore gravity forces are dominant. The effect of including the surface energy becomes obvious only when looking at supercritical flows, where waves are much smaller and capillary forces become more important. Here the extended model provides much better results than

the previous one of Stäbler [6]. However, both models show some deviation from the experiment in the region of the wave crest. Probably, this is not an issue of the models, but of the experimental data, since only data of the liquid phase is available in the wave region. Thus, turbulent kinetic energy might be to low and, therefore, the void profile to steep according to eqn. (21).

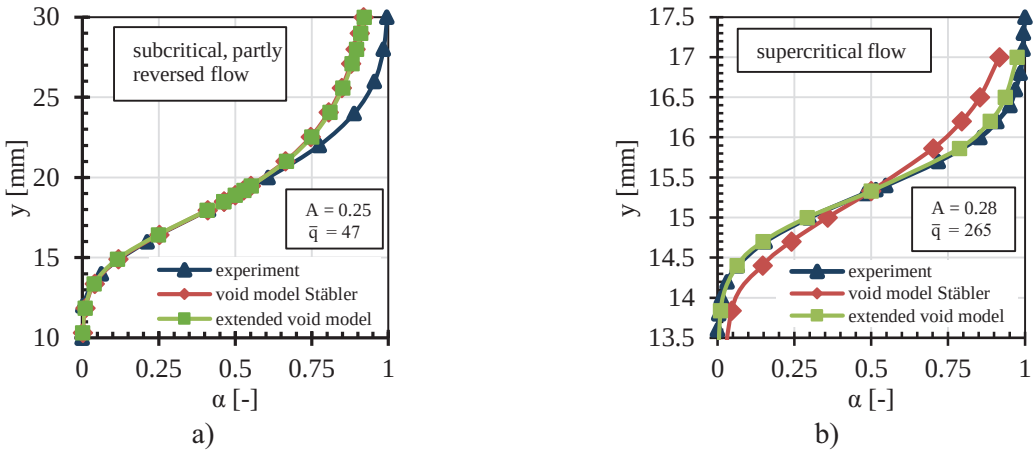

Figure 1. Void distribution calculated by the void models, a) subcritical, partly reversed flow, b) supercritical flow

3. TURBULENCE MODEL

In general, two-phase flows can be solved with the two-fluid formulation in which the mass, momentum and energy equations are solved separately for each phase. Interfacial transfer is considered by exchange terms. Appropriate exchange models are of great importance for good simulation results. Thus, these models are always a big element of uncertainty. If one wants to avoid the necessity of transfer models, the homogeneous two-phase formulation might be an appropriate alternative. Here both fluids share the same flow field, which implies that the velocities of both phases must be equal at the interface. For stratified flows with wave interfaces, this assumption is reasonable because air velocity is slowed down nearly to liquid velocity in the wave troughs. Of course, interfacial transport must be considered as well, which can be done by including interfacial and wave effects in the turbulence model, for example. This is done in this study.

3.1. Governing Equations

According to Rusche [17], the volume-of-fluid solver InterFoam of the open source CFD-tool OpenFOAM 2.2.0 is based on the homogeneous two-phase model. Thus, only one single momentum equation is solved for both phases:

$$\frac{\partial \rho \vec{U}}{\partial t} + \vec{\nabla} \cdot \left(\rho \left[\vec{U} \otimes \vec{U}\right]\right) = -\vec{\nabla} p + \vec{\nabla} \cdot \tau + \rho \vec{g} + \sigma \kappa \vec{\nabla} \alpha \tag{25}$$

Here $\vec{U}$ is the velocity vector, ρ is the density, p and τ are the pressure and the stress tensor respectively, $\vec{g}$ is the gravitational acceleration and $\sigma \kappa \vec{\nabla} \alpha$ the surface tension force according to Brackbill et al. [18]. The density ρ is defined as a density of the mixture of both phases:

$$\rho = \alpha\rho_G + (1-\alpha)\rho_L \tag{26}$$

The different phases are represented by the void fraction α (0: liquid, 1: gas), for which a separate transport equation is solved:

$$\frac{\partial \alpha}{\partial t} + \vec{U} \cdot \vec{\nabla}\alpha = 0 \tag{27}$$

3.2. Turbulence Modeling

As mentioned in section 1, the two-layer turbulence approach is an easy way to include interfacial effects, such as the influence of surface waves. In this model the turbulent eddy viscosity is calculated as:

$$\nu_t = C_\mu \sqrt{k} l_\mu \tag{28}$$

with different turbulent length scales l_μ for the inner and the outer region, as defined by Berthelsen and Ytrehus [10]. Different from this approach, however, the amplitude of the wave (=0.5*H*) according to eqn. (22) is used to predict the turbulent length scale for the inner wavy region.

For the turbulent kinetic energy, the same transport equation as for the k-ϵ or the k-ω turbulence model is solved:

$$\frac{\partial \rho k}{\partial t} + \vec{\nabla} \cdot \left(\rho \vec{U} k\right) - \vec{\nabla} \cdot \left(\rho \left(\nu + \frac{\nu_t}{\sigma_k}\right) \vec{\nabla} k\right) = \rho P - \rho \epsilon \tag{29}$$

where k is the turbulent kinetic energy, ϵ is the dissipation rate of k, ν is the kinematic viscosity of the form $\nu = \alpha\nu_G + (1-\alpha)\nu_L$. ν_t is the turbulent eddy viscosity and P is the turbulence production term.

The upper and lower limits of the inner region are defined as the distance $C_L H$ on the liquid side and $C_G H$ on the gas side of the time averaged position y_M of the interface ($y_M - C_L H \leq y \leq y_M + C_G H$). The constants $C_L = 0.5$ and $C_G = 4.0$ have been determined from a sensitivity study as described by Benz et al. [16]. In the outer regions, where the flow is only single-phase liquid or gas, the two-phase k-ϵ-model or the two-phase k-ω *SST* model is applied.

4. RESULTS

For validation of the new two-layer turbulence model, three different data points from the experiments of Stäbler [6] have been simulated in a two-dimensional model of the channel geometry, one in subcritical, one in supercritical and one in partly reversed flow regime, respectively. The test section investigated by Stäbler is a horizontal duct of 470 mm of length and 90 mm of height (see Fig. 4). The working fluids are air and water at ambient conditions. The inlet flow rates for the different flow regimes and the wave aspect ratios *A*, which were taken from the measurements, are shown in Table I. From a mesh sensitivity study, a mesh with 8995 cells was found to be a good compromise between accuracy and simulation time. Note that parts of the inlet and outlet zones were also included in the simulated geometry.

Table I. Inlet conditions

Data point	Flow regime	Q_L [l/min]	Q_G [l/s]	A [-]
1	subcritical	16.4	39.7	0.10
2	partly reversed	16.6	89.1	0.25
3	supercritical	41.6	39.6	0.25

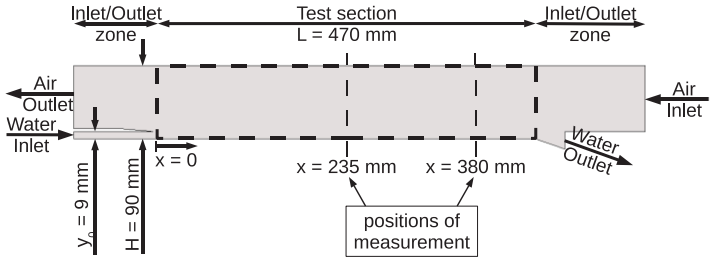

Figure 4. Geometry of the stratified flow experiment of Stäbler [6].

In the following sections, simulation results of the standard two-phase k-ϵ-model and the new two-layer turbulence model are discussed exemplarily for a subcritical (data point 1) and for a partly reversed flow (data point 2). Results in supercritical flow have been shown recently in Benz et al. [16]. The results are taken at the horizontal position x = 235 mm downstream of the liquid inlet.

4.1. Subcritical Flow

Fig. 5a) shows the void-distribution profiles for subcritical flow. Both simulations with the two-layer model are in good agreement with the experiment, while the two-phase k-ϵ-model slightly overestimates the water depth. From the velocity distributions, shown in Fig. 5b), it can be seen that only the two-layer together with the k-ϵ-model is able to predict the velocity profiles accurately. Using the standard k-ϵ-model clearly gives different results compared to the experimental data. Looking at the turbulent kinetic energy in Fig. 5c) and d), both two-layer approaches shows again better agreement with the experiment. While the k-ω *SST* formulation of the two-layer model is better in the wall regions, the k-ϵ formulation gives better results near the interface. Nonetheless, there is still some deviation near the surface. Unfortunately, the gas phase turbulence could not be measured in the wavy region. But from the results of Lorencez et al. [5], where turbulent fluctuations were also ejected at the interface, we assume that the predicted increase of turbulent kinetic energy at the interface, as calculated by the two-layer k-ϵ-model, is physically meaningful.

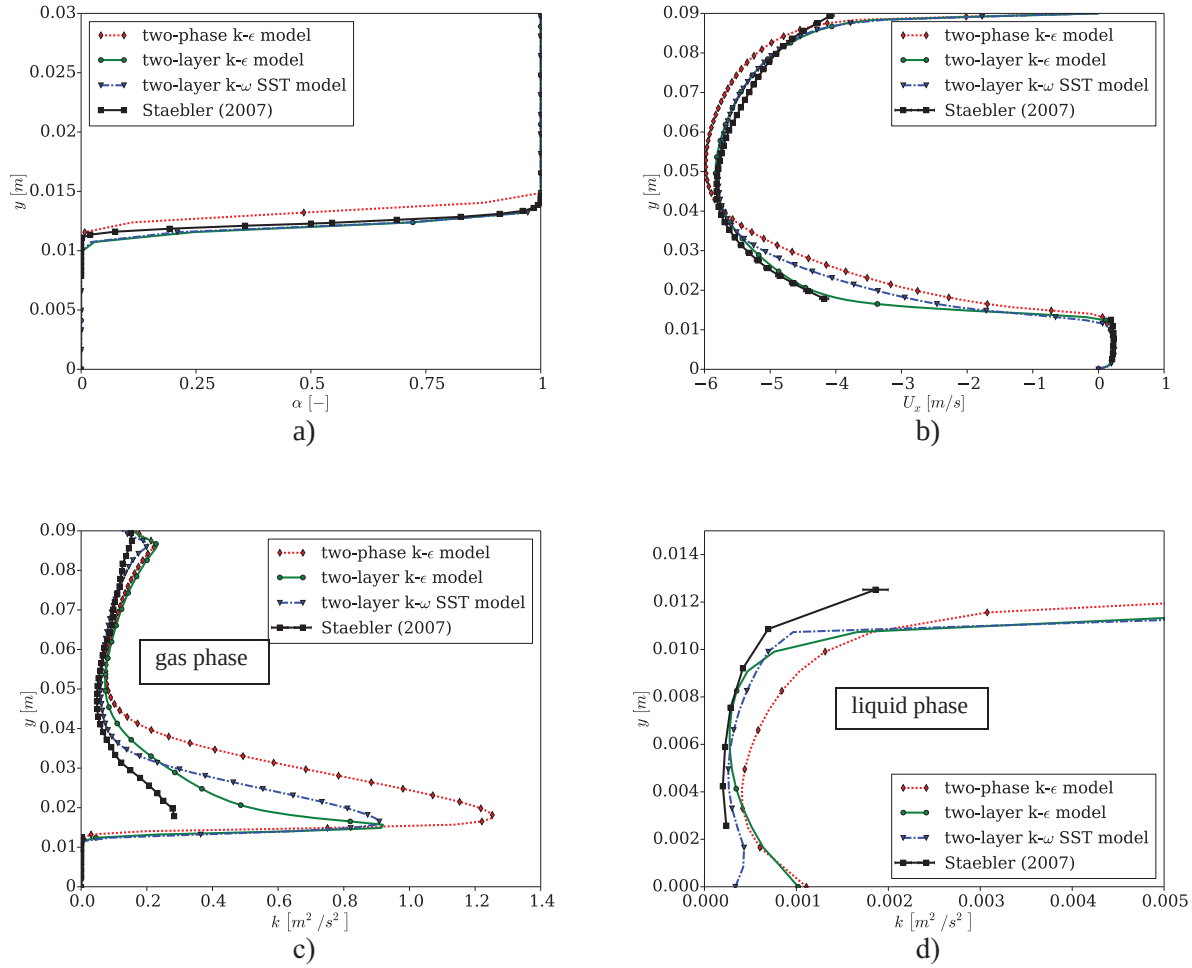

Figure 5. Void profiles (a), velocity profiles (b) and turbulent kinetic energy profiles (c, d) in subcritical flow

4.2. Partly Reversed Flow

Here only simulations with the two-layer k-ϵ-model are shown, since those with the two-layer *k-ω SST* model were not yet available at the time of paper submission. It is apparent from the void distribution in Fig. 6a) that only the two-layer approach is able to reflect the measured void profile, with little overestimation of the liquid height. Even the slope and therefore the height of the waves are calculated accurately. The model underestimates only the deepness of the wave troughs in the region of low void. The interface predicted by the two-phase k-ϵ-model appears to be too smooth. Like for subcritical flow, the velocity profile predicted by the two-layer model agrees much better with measurements than the one calculated by the two-phase k-ϵ-model (see Fig. 6b)). A clear improvement due to the new turbulence model compared with the two-phase k-ϵ-model can be seen when looking at the turbulent kinetic energy of the gas phase in Fig. 6c). While the k-ϵ-model overestimates the turbulent energy, the two-layer turbulence approach predicts almost exactly the turbulent kinetic energy profile in the gas phase, in particular in the region near the interface. In the liquid phase, however, the k-ϵ-model gives better results (Fig. 6d). The reason for different kinetic energies between y = 0.012 m and y = 0.021 m is their different definition in the simulation compared to the experiment. While only the liquid phase was measured in the

experiment, we have the turbulent kinetic energy of the homogenous flow in the simulation according to section 2.1.. Thus, results are not comparable in the wavy region where $0 < \alpha < 1$.

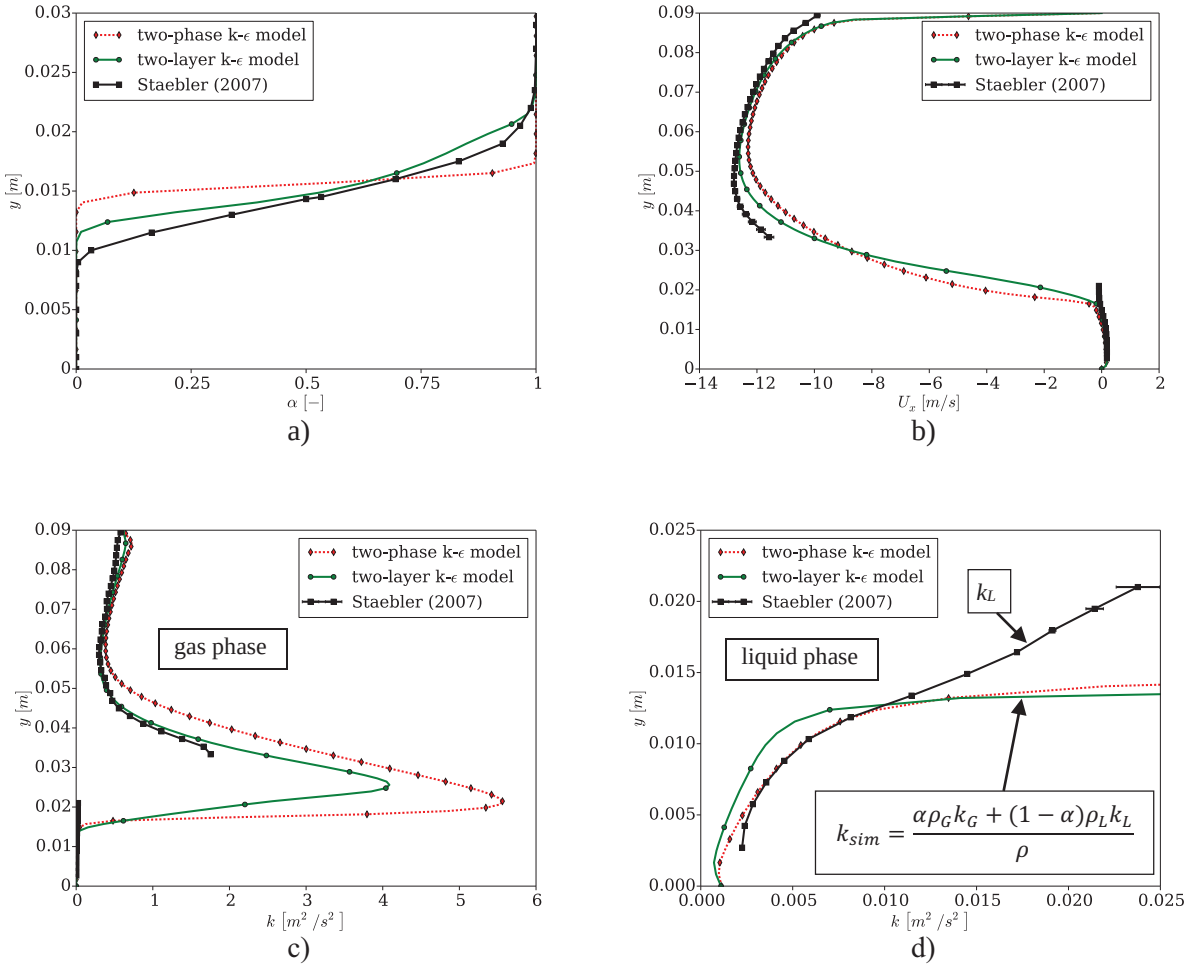

Figure 6. Void profiles (a), velocity profiles (b) and turbulent kinetic energy profiles (c, d) in partly reversed flow

5. CONCLUSIONS

Different from former turbulence models for wavy interfaces, we tried to derive a new model based on a solid physical basis. Based on energy statistics, we developed a model, which is able to describe complete wave spectra. We found that the spectrum of wave numbers, eqn. (8), is independent of the flow regime, and thus similar for supercritical and for subcritical flow. Information about the phase velocity of waves is needed only if frequency spectra shall be used for validation. Otherwise, such information does not enter into the turbulence model, which reduces the number of uncertainties significantly. Using this statistical model instead of drag and lift forces between gas and liquid phases together with the two-layer approach, we got a simple turbulence model for a homogeneous two-phase flow, which needs a minimum of fitting parameters, i.e. C_L and C_G only. The new turbulence model shows good agreement in the description of the time averaged void and velocity profiles in the wavy zone. Although prediction of turbulent kinetic energy

profiles is in better agreement compared to the standard k-ϵ-model, the new model still shows some deviation to experimental data. Therefore, further validation analyses are planned to refine the new model.

REFERENCES

[1] M. Rashidi, G. Hetsroni, S. Banerjee, "Mechanisms of heat and mass transport at gas-liquid interfaces", *Int. J. Heat Mass Transfer*, **34**, pp. 1799-1810 (1991).

[2] S. Komori, H. Ueda, F. Ogino, T. Mizushina, "Turbulence structure and transport mechanism at the free surface in an open channel flow", *Int. J. Heat Mass Transfer*, **25**, pp. 513-521 (1982).

[3] M. Rashidi and S. Banerjee, "Turbulence structure in free-surface channel flows", *Physics of Fluids*, **31**, pp. 2491-2503 (1988).

[4] M. Rashidi, G. Hetsroni, S. Banerjee, "Wave-turbulence interaction in free-surface channel flows", *Physics of Fluids A*, **4**, pp. 2727-2738 (1992).

[5] C. Lorencez, M. Nasr-Esfahany, M. Kawaji, M. Ojha, "Liquid turbulence structure at a sheard and wavy gas-liquid interface", *Int. J. Multiphase Flow*, **23**, pp. 205-226 (1997).

[6] T.D. Stäbler, *Experimentelle Untersuchung und physikalische Beschreibung der Schichtenströmung in horizontalen Kanälen*, PhD Thesis, Sc. Report FZKA 7296, Forschungszentrum Karlsruhe GmbH, Karlsruhe, Germany, 2007.

[7] M. Gargallo, T. Schulenberg, L. Meyer, E. Laurien, "Counter-current flow limitations during hot let injection in pressurized water reactors", *Nucl. Eng. Des.*, **235**, pp. 785-804 (2005).

[8] B.T. Daly and F.H. Harlow, "A Model of Countercurrent Steam-water Flow in Large Horizontal Pipes", *Nucl. Sci. Eng.*, **77**, pp. 273-284 (1981).

[9] M. Akai, A. Inoue, S. Aoki, "The prediction of stratified two-phase flow with a two-equation model of turbulence", *Int. J. Multiphase Flow*, **7**, pp. 21-39 (1981).

[10] P.A. Berthelsen and T. Ytrehus, "Calculations of stratified wavy two-phase flow in pipes", *Int. J. Multiphase Flow*, **31**, pp. 571-592 (2005).

[11] H.C. Chen and V.C. Patel, "Near-Wall Turbulence Models for Complex Flows Including Separation", *AIAA Journal*, **26**, pp. 641-648 (1988).

[12] T. Höhne, J.-P. Mehlhoop, "Validation of closure models for interfacial drag and turbulence in numerical simulations o horizontal stratified gas-gliquid flows", *Int. J. Multiphase Flow*, **62**, pp. 1-16 (2014).

[13] J. Fabre, L. Masbernat, C. Suzanne, "EXPERIMENTAL DATA SET NO. 7: STRATIFIED FLOW, PART I: LOCAL STRUCTURE", *Multiphase Sci. Technol.*, **3**, pp. 285-301 (1987).

[14] C. Vallée, T. Höhne, H.-M. Prasser, T. Sühnel, "Experimental investigation and CFD simulation of horizontal stratified two-phase flow phenomena", *Nucl. Eng. Des.*, **238**, pp. 637-646 (2008).

[15] T. Wintterle, E. Laurien, T. Stäbler, L. Meyer, T. Schulenberg, "Experimental und numerical investigation of counter-current stratified flows in horizontal channels", *Nucl. Eng. Des.*, **238**, pp. 627-636 (2008).

[16] M. Benz, T. Schulenberg, "Validation analyses of advanced turbulence model approaches for stratified two-phase flows", *Comp. Meth. Multiphase Flow VIII*, **89**, pp. 361-372 (2015).

[17] H. Rusche, *Computational fluid dynamics of dispersed two-phase flows at high phase fractions*, PhD Thesis, Imperial College of Science, Technology and Medicine, London, GB (2002).

[18] J.U. Brackbill, D.B. Kothe, C. Zemach, "A continuum method for modelling surface tension", *J. of Comp. Physics*, **100**, pp. 335-354 (1992).